

Pullout Load Capacity of a Circular Earth Anchor Buried in Sand

WALLACE H. BAKER and ROBERT L. KONDNER

Respectively, Graduate Student and Associate Professor of Civil Engineering,
Northwestern University

The results of pullout load capacity tests performed on numerous small-scale model earth anchors are presented. The techniques of dimensional analysis are used to develop empirical relationships among anchor size, depth of anchor embedment, and pullout capacity for single anchors of circular cross-section buried in a dense uniform sand. A distinction is made between shallow and deep anchors. The range of the ratio of depth of embedment to anchor diameter studied corresponds to the general range found in field applications of earth anchors that are used to provide tieback resistance for retaining structures and uplift resistance for transmission towers, utility poles, moorings, etc. The results of two full-scale field tests of Webb-Lipow type anchors are also reported.

•THIS INVESTIGATION presents the results of pullout load capacity tests performed on numerous small-scale model earth anchors. The range of the ratio of depth of embedment to anchor diameter (h/d) studied corresponds to the general range found in field applications of earth anchors.

The purpose of the investigation was to develop an empirical relationship among the depth of anchor embedment, anchor width, and pullout capacity of earth anchors, and to define the transition point from a shallow failure to a deep failure for increasing depth of embedment. The study was limited to tests performed on single anchors of circular cross-sectional shape buried in a dense uniform sand. The results of pullout load capacity tests performed on two full-scale field earth anchors of the Webb-Lipow type are also reported.

Earth anchors are used to provide uplift resistance for transmission towers (1, 2), utility poles, aircraft moorings, submerged pipelines (3) and tunnels (4), and to develop the tieback forces required to eliminate external bracing from retaining structures and sheeting walls (5, 6, 7, 8). The use of earth anchors in specific projects has been limited by a number of factors including the lack of economical methods of in-place construction, the absence of a rational approach to the design of earth anchor systems (9), and the general unfamiliarity of the industry with the possible uses of earth anchors.

Although several types of prefabricated earth anchors are commercially available, they cause serious disturbance to the surrounding soil during installation. The effect of such soil disturbance may be a major reduction in the pullout capacity of the anchor. To take full advantage of the natural strength of the soil, an anchor should be constructed in place without disturbing the soil. Anchors can be constructed in place in the following manner: first, a small-diameter shaft is drilled to the necessary depth; next, an expandable reaming device is used to enlarge the bottom of the shaft hole to the desired diameter; and finally, the enlarged hole is filled with concrete and reinforcing steel to form the required anchorage (7).

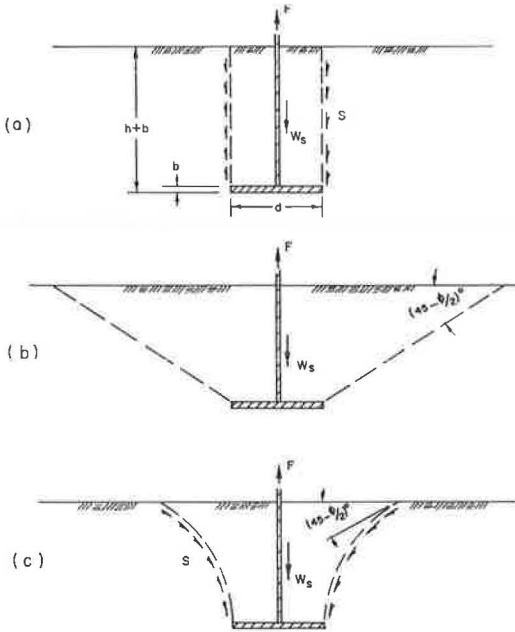


Figure 1. Methods for calculating pullout load capacity for earth anchors: (a) friction cylinder method, (b) soil cone method, and (c) Balla's method.

Present methods for calculating the pullout capacity of anchors in sand are based on an assumed shape for the failure surface and, with the exception of Balla's (10) method, give results contrary to those observed.

The friction cylinder method (earth pressure method, Swiss formula, Frohlich-Majer's procedure, 10) assumes that failure occurs along the surface of a cylinder of soil above the anchor. The cylinder has the same cross-section as the horizontal projection of the anchor (Fig. 1a). The pullout capacity is computed by considering the weight of the cylinder of soil and the frictional resistance along its surface.

The weight-of-cone method (earth load method, Mohr's formula, 10) assumes that the failure surface takes the shape of a truncated cone extending above the anchor with an apex angle of $90 + \phi$ (Fig. 1b). The pullout capacity is given as the weight of the soil within the truncated cone.

The method presented by Balla (10) is based on the shape of the failure surface observed during small-scale model anchor tests (Fig. 1c) in sand. Applying Kötter's equation to this failure surface,

he computed the theoretical pullout capacity for circular anchors and showed it to be proportional to the third power of the depth of embedment. Such a theoretical analysis gives adequate correlation with Balla's small-scale model anchor tests, the model tests conducted in this study for a h/d ratio less than 6, several field tests of shallow anchors reported by Balla, and the shallow field test reported herein. According to the results of the present study, however, when extended to a h/d ratio greater than 6, Balla's method gives a pullout capacity greater than that actually developed. Thus, his method should not be considered applicable to deep anchors.

DIMENSIONAL ANALYSIS

Dimensional analysis, formalized by Buckingham (11) in his well-known π -theorem, has been used by numerous researchers to determine the functional relationships between the primary physical constants involved in physical phenomena. In this respect, dimensional analysis is often helpful in providing a simple basis for the possible correlation of the results of small-scale model tests with the behavior of full-scale prototypes.

According to the π -theorem, a physical phenomenon which is a function of n physical quantities involving m fundamental units can be described in the following functional form:

$$F(\pi_1, \pi_2, \dots, \pi_{n-m}) = 0 \quad (1)$$

where the π -terms are the $(n - m)$ independent dimensionless products of the n physical quantities (6).

The primary physical quantities for the pullout capacity of a flat anchor buried in sand are listed in Table 1 using the force, length, and time system of fundamental units.

TABLE 1
PRIMARY PHYSICAL QUANTITIES USED IN DIMENSIONAL ANALYSIS OF A FLAT CIRCULAR ANCHOR EMBEDDED IN SAND

Physical Quantity	Symbol	Fundamental Units
Pullout load capacity	F	F
Cross-sectional area of anchor	A	L ²
Perimeter of anchor	c	L
Thickness of anchor	b	L
Depth of embedment	h	L
Unit weight of soil	γ	FL ⁻³
Angle of internal friction	ϕ	F ⁰ L ⁰ T ⁰
Relative density	D _d	F ⁰ L ⁰ T ⁰
Void ratio	e	F ⁰ L ⁰ T ⁰
Time of loading	t	T
Rate of loading	r	FT ⁻¹

By appropriate manipulations, the eleven physical quantities yield the following eight π -terms: $\pi_1 = F/h\alpha\gamma$, $\pi_2 = h^2/A$, $\pi_3 = c/b$, $\pi_4 = \gamma hA/rt$, $\pi_5 = c^2/A$, $\pi_6 = \phi$, $\pi_7 = D_d$, and $\pi_8 = e$. For this set of π -terms, Eq. 1 implies the functional relation:

$$F/h\alpha\gamma = f_1 \left(h^2/A, c/b, \gamma hA/rt, c^2/A, \phi, D_d, e \right) \quad (2)$$

By additional algebraic transformations, an alternate set of independent π -terms can be obtained which yields the functional relation:

$$F/c^3\gamma = f_2 \left(h/c, c/b, \gamma hA/rt, c^2/A, \phi, D_d, e \right) \quad (3)$$

For anchors of circular cross-section, with diameter d , the following simplification of π -terms is possible: $F/h\alpha\gamma \rightarrow F/hd^2\gamma$, $F/c^3\gamma \rightarrow F/d^3\gamma$, $\gamma hA/rt \rightarrow \gamma hd^2/rt$, $c^2/A \rightarrow 4\pi$.

By varying the rate of loading, the dimensionless parameter $\gamma hd^2/rt$ can be kept relatively constant and, hence, its effects can be minimized. The flow characteristics or viscosity of the sand is assumed to be a function of the soil properties γ , ϕ , D_d , and e and, therefore, is not considered an independent variable.

If all tests are conducted in the same sand at a constant density, the parameters ϕ , D_d , and e can be considered constants. Subject to the preceding restrictions, Eqs. 2 and 3 reduce to:

$$F/hd^2\gamma = g_1 (h^2/d^2, d/b) \quad (4)$$

and

$$F/d^3\gamma = g_2 (h/d, d/b) \quad (5)$$

respectively. The explicit forms of Eqs. 4 and 5 must be determined by experiment.

EXPERIMENTAL PROCEDURE

The model anchors for this study were flat circular $\frac{1}{4}$ -in. thick steel plates with diameters of 1.00, 1.50, 2.00, and 3.00 in. An 0.078-in. diameter straight piano wire was inserted in the center of each anchor to serve as a tie rod. The model tests were conducted at depths of embedment of 3.0, 6.0, 9.0, 12.0, 15.0, 18.0, and 21.0 in.

A schematic drawing of the loading system is shown in Figure 2. Vertical load was applied to the anchor in increments through a cable and pulley system with a swivel joint inserted between the tie rod connection and the cable to allow the cable to twist. Movement of the anchor was measured by a reverse-reading deflection dial mounted on a reference beam.

The model anchor tests were conducted in an air-dry uniform silica sand (ASTM 20-30 Ottawa sand) with the following properties: specific gravity, $G = 2.66$; angle of internal friction, $\phi = 42$ deg; average unit weight, $\gamma_{avg.} = 112.1$ pcf. The unit weight ranged from 111.8 to 112.5 pcf for all tests.

The sand was placed in a metal tank through a No. 12 U. S. standard sieve held 20 to 30 in. above the surface of the sand. The sieve was moved slowly back and forth across the tank in a rectangular grid pattern. When the sand was at the desired depth below the top of the tank, the anchor was carefully set in place, and the sieving operation continued to the top of the tank. The sand was weighed after the test to compute the average unit weight.

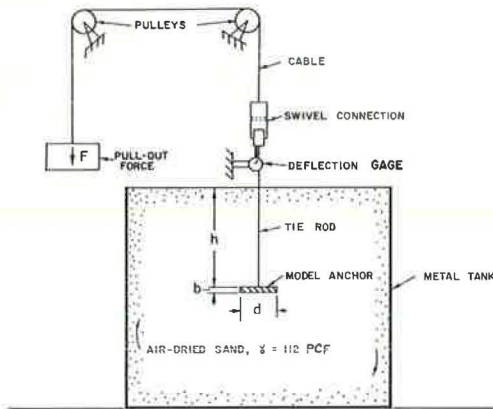


Figure 2. Test setup and loading apparatus for model anchor tests.

To study the shape of the failure surface developed for shallow and deep anchors, supplemental anchor tests were conducted in a clear plexiglass tank containing colored sand strata. The tank was made of $\frac{1}{2}$ -in. plexiglass screwed and glued together to form an open-top box 35 by 7 in. in plan and 22 by 35 in. in profile. The anchors used were flat steel plates measuring 7.0 by 1.0, 2.0, and 3.0 in., respectively.

The colored sand layers for the tests were made by placing a thin layer of black (dyed) ASTM 20-30 Ottawa sand against the front wall of the tank at 1-in. vertical intervals. Loads were applied until a failure surface developed or until the anchor was pulled out the tank.

EXPERIMENTAL RESULTS

The experimental data for the model anchor tests conducted in this study are given in Table 2. The average value of pullout capacity vs depth is plotted for each anchor diameter in Figure 3.

The pullout capacity was defined as the smallest load causing a disproportionate movement of the anchor. For the majority of tests, the pullout capacity was the maximum load resistance attained by the anchor. However, for a few tests the first large movement of the anchor was followed by a small increase in load resistance.

For the few cases having this type of load-deflection response, the h/d 's were all equal to or greater than 6. A typical example of this type of load-deflection response is shown in Figure 4.

For shallow anchors ($h/d < 6$), a definite failure circle was observed to develop on the surface of the sand as the anchor system failed (Fig. 5a). For deep anchors ($h/d \geq 6$), however, only a slight rise in the surface of the sand occurred in the vicinity of the tie rod at failure.

The 3-in. wide anchor tested at a depth of 14-in. in the plexiglass tank developed a definite failure surface (Fig. 5b) similar in shape to that proposed by Balla (10). The 1- and 2-in. wide anchors tested at the same depth in the plexiglass tank did not produce a visible failure surface until the anchor had been pulled to within a few inches of the surface and was acting as a "shallow" anchor.

TABLE 2
EXPERIMENTAL DATA—MODEL TESTS

Test No.	Depth, h (in.)	Diameter, d (in.)	Pullout Capacity, F (lb)	Radius of Failure Circle (in.)	Unit Weight, γ_t (pcf)
1	3	1.0	2.2	2.15	—
2	3	1.0	2.2	2.30	112.09
3	6	1.0	12.6	—	—
4	6	1.0	11.0	—	111.96
5	9	1.0	32.9	—	111.91
6	12	1.0	52.9	—	—
7	12	1.0	55.6	—	112.30
8	15	1.0	81.6	—	112.44
9	18	1.0	110.2	—	111.93
10	18	1.0	79.4	—	112.47
11	21	1.0	130.1	—	111.76
12	9	1.5	35.7	—	112.33
13	12	1.5	66.1	—	112.27
14	12	1.5	72.8	—	—
15	15	1.5	105.8	—	111.93
16	18	1.5	141.1	—	112.33
17	3	2.0	3.5	2.45	—
18	6	2.0	15.4	4.20	—
19	6	2.0	15.4	4.00	—
20	9	2.0	39.7	—	112.04
21	12	2.0	79.4	—	—
22	15	2.0	138.9	—	111.82
23	15	2.0	138.9	—	112.19
24	18	2.0	200.7	—	—
25	21	2.0	247.0	—	111.99
26	21	2.0	211.7	—	—
27	3	3.0	5.5	4.35	—
28	6	3.0	17.9	4.60	—
29	9	3.0	49.6	6.25	112.04
30	9	3.0	49.0	6.60	—
31	12	3.0	95.3	8.00	111.93
32	15	3.0	167.6	—	111.82
33	18	3.0	273.4	—	111.88
34	18	3.0	264.6	—	112.19
35	21	3.0	388.1	—	111.79

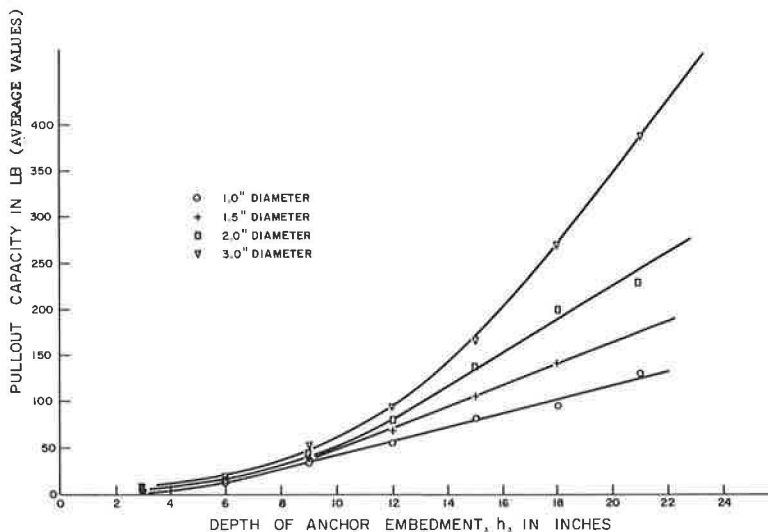


Figure 3. Plot of anchor pullout capacity vs depth of anchor embedment.

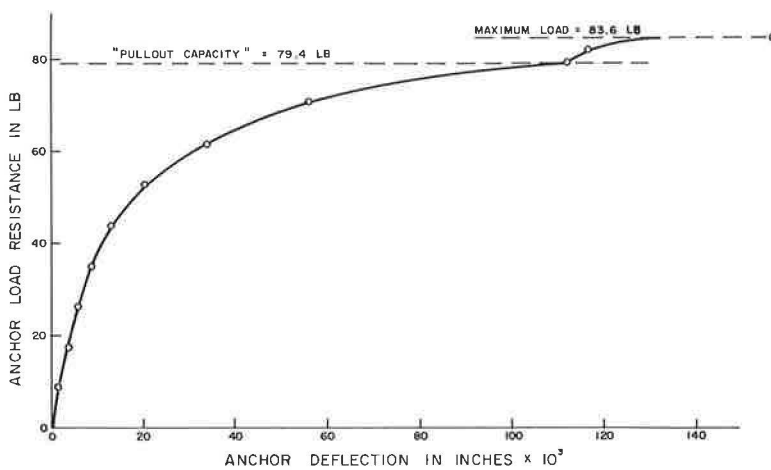


Figure 4. Load vs deflection curve for model test No. 21.



(a)



(b)

Figure 5. (a) failure circle developed by shallow anchor ($h/d < 6$); and (b) shape of two-dimensional failure surface developed by 3-in. wide anchor.

DISCUSSION OF RESULTS

The appearance of a failure circle on the sand surface only for shallow anchors ($h/d < 6$) indicates a difference in the mode of failure between deep and shallow anchors. This difference would logically be represented by two distinct functional equations relating the primary quantities.

The test results shown in Figure 3 are plotted in Figure 6 in terms of the dimensionless parameters $F/hd^2\gamma$ and h^2/d^2 . For the range $h/d < 6$, the curve in Figure 6 appears to be insensitive to changes in the parameter d/b . This portion of Figure 6 is plotted in Figure 7 and can be approximated by a straight line. Thus Eq. 4 has the form, for $h/d < 6$:

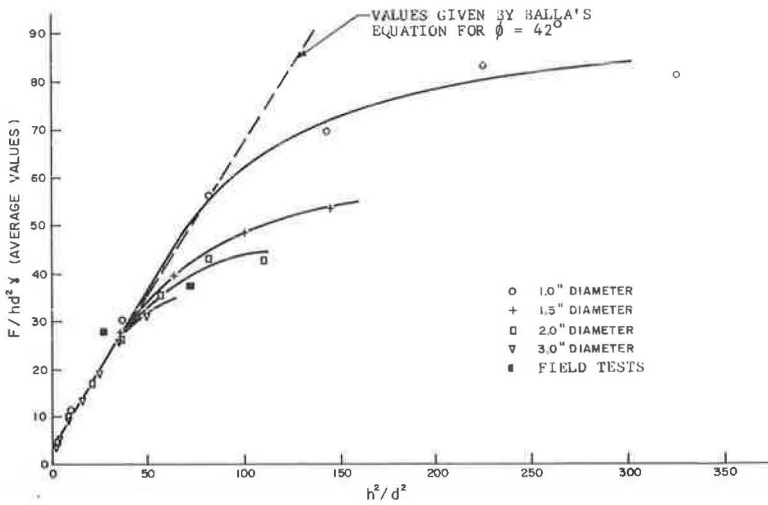


Figure 6. Plot of $F/hd^2\gamma$ vs h^2/d^2 .

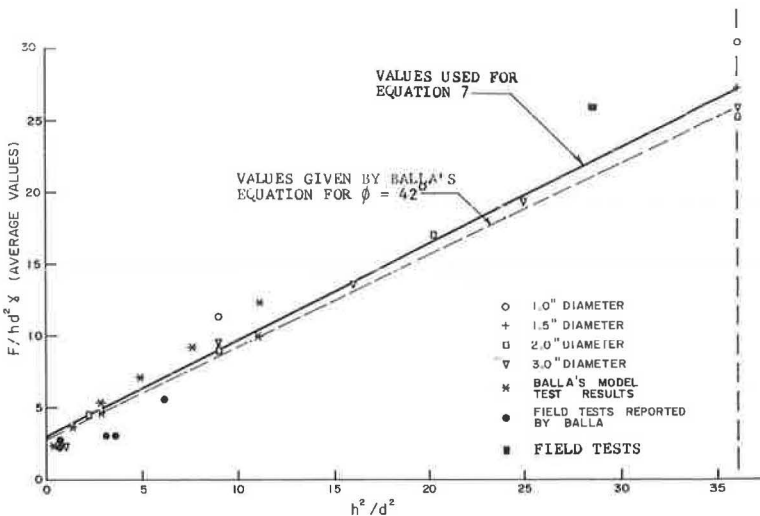


Figure 7. Plot of $F/hd^2\gamma$ vs h^2/d^2 for $h/d \leq 6$.

$$F/hd^2\gamma = C_1 + C_2h^2/d^2 \quad (6)$$

where C_1 is the intercept and C_2 is the slope of the straight-line portion of the curve in Figure 7. Solving for the pullout capacity yields, for $h/d < 6$:

$$F = C_1hd^2\gamma + C_2h^3\gamma \quad (7)$$

where $C_1 = 3.0$ and $C_2 = 0.67$ for the particular values of ϕ , D_d , and e used. The constants C_1 and C_2 are presumably functions of ϕ and D_d . Such an assumption allows Eq. 7 to be written in the form

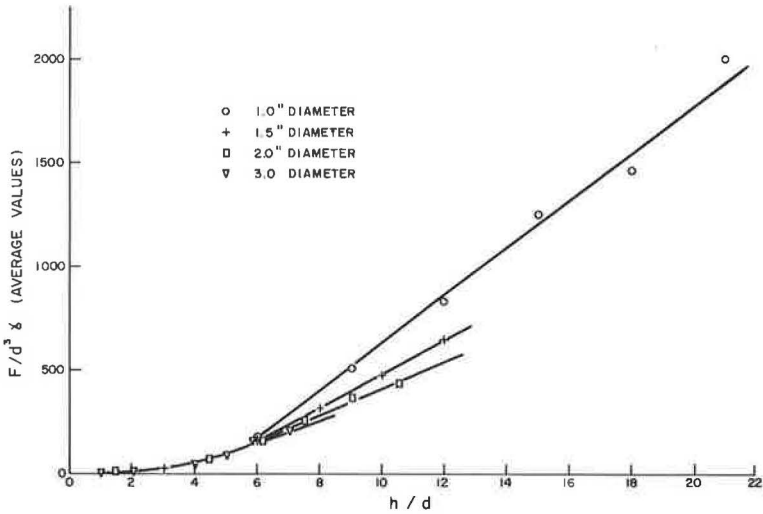


Figure 8. Plot of $F/d^3\gamma$ vs h/d .

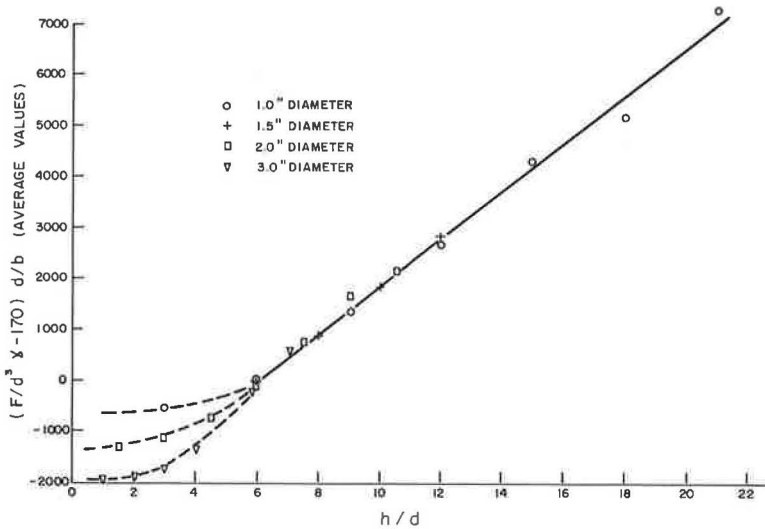


Figure 9. Plot of parameters $(F/d^3\gamma - 170) d/b$ vs h/d .

$$F = h^3 \gamma \left[H_1(\phi, D_d) + H_2(\phi, D_d) \left(d^2/h^2 \right) \right] \quad (8)$$

for $h/d < 6$. Eq. 8 is similar in form to Balla's equation for circular anchors in cohesionless soil (10) which can be written:

$$F = h^3 \gamma \left[H_1(\phi, h/d) + H_2(\phi, h/d) \right] \quad (9)$$

Balla's results have been plotted in Figure 7 in dimensionless form. Use of Eqs. 8 or 9 gives pullout capacities larger than those actually observed in the model tests for $h/d > 6$, as shown in Figure 6.

Because the thickness, b , of the anchor does not appear in either Eq. 7 or Balla's equation, these equations do not apply to anchors with small values of d/b (e.g., $d/d < 1$) since such anchors act primarily as friction piles.

The test results are plotted in terms of the alternate dimensionless parameters $F/d^3\gamma$ and h/d in Figure 8. The parameter $F/d^3\gamma$ is a function of d/b for $h/d > 6$ and converges to $F/d^3\gamma = 170$ for $h/d = 6$.

If the origin in Figure 8 is moved upwards to $F/d^3\gamma = 170$ and the ordinate is then multiplied by d/b , the several curves shown for $h/d > 6$ in Figure 8 reduce to the single curve shown in Figure 9. For the range $h/d \geq 6$, the curve in Figure 9 can be approximated by a straight line. Thus, Eq. 5 has the modified form, for $h/d \geq 6$:

$$\left(F/d^3\gamma - 170 \right) d/b = C_3 + C_4 h/d \quad (10)$$

where C_3 is the intercept and C_4 is the slope of the curve in Figure 9. Solving Eq. 10 for the pullout capacity yields, for $h/d \geq 6$:

$$F = 170 d^3\gamma + C_3 d^2 b \gamma + C_4 h d b \gamma \quad (11)$$

where $C_3 = 2,800$ and $C_4 = 470$ for the particular values of ϕ , D_d , and e used.

Because of the limited range of d/b values included in this study, it was not possible to determine whether Eq. 11 is applicable to anchors with values of $d/b < 4$.

The equations presented herein for the pullout capacity of a circular anchor buried in sand are based entirely on the results of small-scale model tests conducted in a specific sand having particular properties. For Eqs. 7 and 11 to be useful in actual design, empirical values for C_1 , C_2 , C_3 , and C_4 must be determined for various values of ϕ and D_d , and must also be correlated with the results of full-scale field tests. The correlation between model and field tests is especially important since the size of the sand grains used in the laboratory cannot be reduced to the same scale as the model anchor. Such a contradiction in the geometrical similitude between the model and the prototype may produce unexpected effects.

FIELD TESTS

Pullout load capacity tests were performed on two full-scale field earth anchors of the Webb-Lipow type buried in a relatively uniform fine sand (dune deposits) at the site of the Redondo Steam Station of the Southern California Edison Co., Los Angeles, Calif. Average soil properties were as follows (13): angle of internal friction, $\phi = 37$ deg; dry unit weight, $\gamma_{dry} = 105$ pcf and in-place unit weight, $\gamma_t = 112$ pcf. Groundwater was encountered at a depth of about 18 ft below the surface.

The anchors were installed and tested by Webb and Lipow, General Engineering Contractors, Los Angeles, Calif. A 5-in. diameter shaft was first drilled and cased to about the desired anchor depth. AM-9 chemical grout was then placed at the bottom of the shaft to stabilize the sand during the subsequent reaming operation. A relatively weak grout was used so that the strength characteristics of the sand would not be significantly changed. Next, an expandable reaming tool fitted to a rotary vacuum drill rig was used to produce a cone-shaped void at the bottom of the shaft. The anchor was formed by filling the void with concrete after a $7/8$ -in. diameter high-strength steel tie

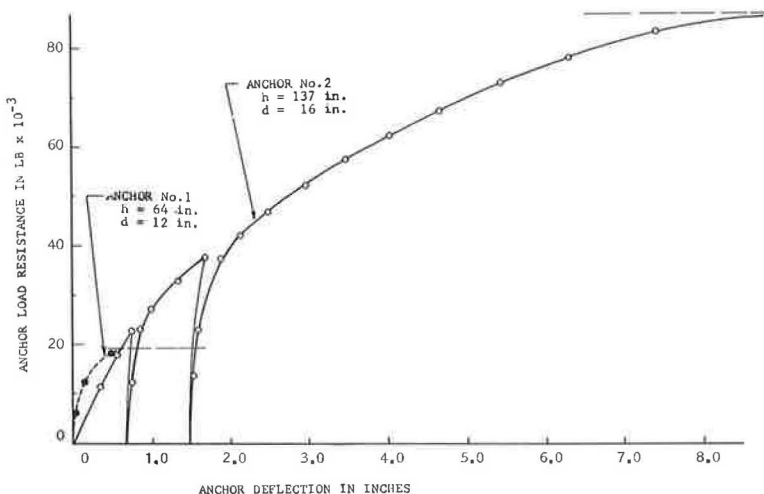


Figure 10. Plot of load vs deflection for field tests.

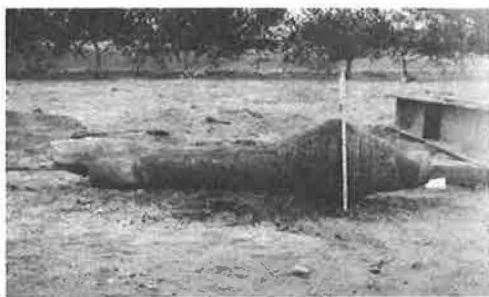


Figure 11. Field anchor No. 2 after testing.

rod had been inserted in the shaft. A special reinforcing device was used at the end of the tie rod to develop bond between the rod and the concrete.

Load was applied to the earth anchors in increments with a calibrated center-hole hydraulic jack supported by two steel reaction beams. Movement of the anchor was measured by a tensioned reference wire read against a scale fastened to the tie rod. Results of the two field tests and the dimensions of the anchors are shown in Figure 10. Figure 11 shows anchor No. 2 after having been pulled out of the ground.

Field test results are plotted in dimensionless form in Figures 6 and 7. The pullout load capacity for the shallow anchor was higher than the values predicted by Eq. 7 and Balla's equation. Since the thickness, b , of the field anchor is indeterminate, a direct comparison between the capacity of the deep anchor and that predicted by Eq. 11 is not justified.

CONCLUSIONS

1. The modes of failure for shallow ($h/d < 6$) and deep ($h/d \geq 6$) anchors in dense sand are distinct and require separate analyses.
2. The pullout capacity for shallow and deep anchors in a dense sand can be represented by Eqs. 7 and 11, respectively.

ACKNOWLEDGMENTS

The authors are indebted to the Walter P. Murphy Fellowship Fund, Northwestern University Computer Center, and the Technological Institute Research Committee for supporting various aspects of the laboratory investigation. Parts of the model study were also conducted as a phase of the research supported under National Science Foundation grant NSF-GP-359.

REFERENCES

1. Giffels, W. C., et al. Concrete Cylinder Anchors Proved for 345-KV Tower Line. *Electrical World*, Vol. 154, pp. 46-49, Dec. 19, 1960.
2. Markowsky, M., and Adams, J. I. Transmission Towers Anchored in Muskey. *Electrical World*, Vol. 155, pp. 36-37, 68, Feb. 20, 1961.
3. Hollander, W. H. Earth Anchors May Help You Prevent Pipe Flotation at River Crossings. *Oil and Gas Jour.*, Vol. 56, pp. 98-101, May 26, 1958.
4. Poland, G. E. Anchoring a Tunnel in Sand. *Civil Eng.* p. 59, March 1960.
5. Belled Caissons Anchor Walls. *Eng. News-Record*, p. 28, May 11, 1961.
6. Cut Slope is Prestressed With Beams and Anchors. *Eng. News-Record*, Vol. 165, pp. 52-53, Oct. 20, 1960.
7. Tiebacks Remove Clutter in Excavation. *Eng. News-Record*, pp. 34-36, June 8, 1961.
8. Tie-Back Wall Braces Building Excavation. *Construction Methods and Equipment*, pp. 116-119, Nov. 1962.
9. Tied-Back Embankment Slides into Excavation. *Eng. News-Record*, p. 23, July 6, 1961.
10. Balla, A. The Resistance to Breaking Out of Mushroom Foundations for Pylons. *Proc. 5th Int. Conf. on Soil Mech. and Found. Eng.*, Vol. 1, pp. 569-576, 1961.
11. Buckingham, E. On Physically Similar Systems. *Phys. Rev.*, Vol. 4, pp. 354-376, 1914.
12. Bridgman, P. W. *Dimensional Analysis*. Connecticut, Yale Univ. Press, 1931.
13. Crandall, Leroy, and Associates, Consulting Foundation Engineers. Report of Foundation Investigation, Proposed Generating Station and Fuel Tank, Redondo Steam Station, Redondo Beach, California, for the Southern California Edison Company. Aug. 7, 1964.